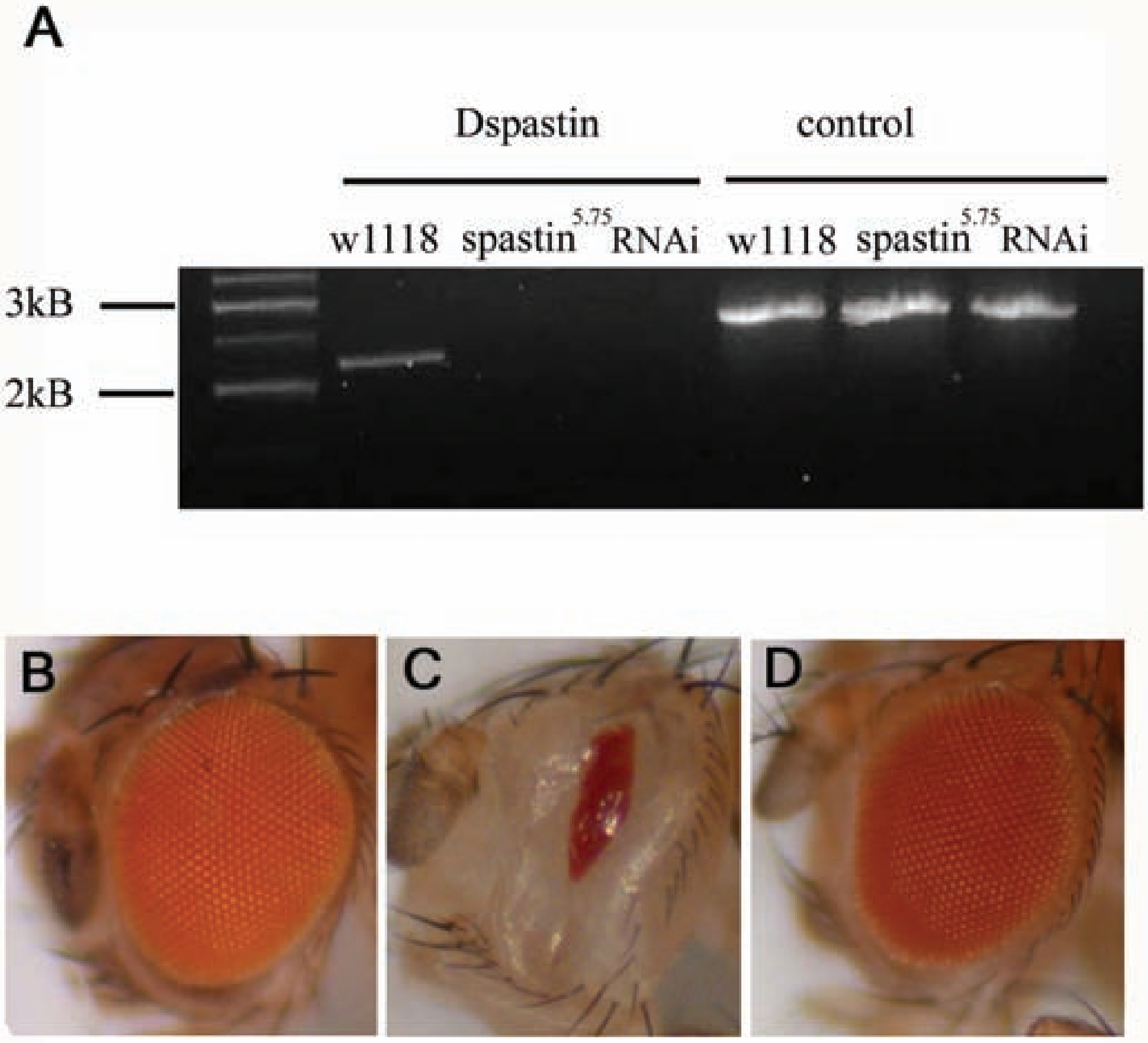
A
Dspastin
control
w1118
spastin5.75 RNAi
w1118
spastin5.75 RNAi
3kB
2kB
B
C
D

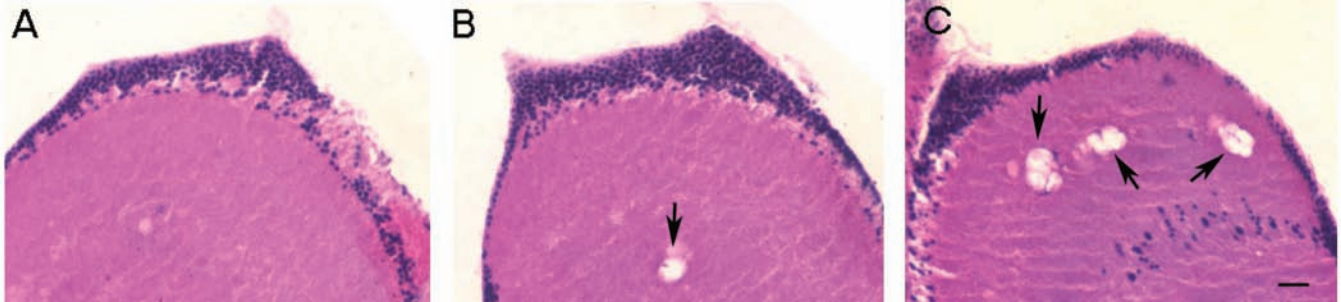
A
B
C

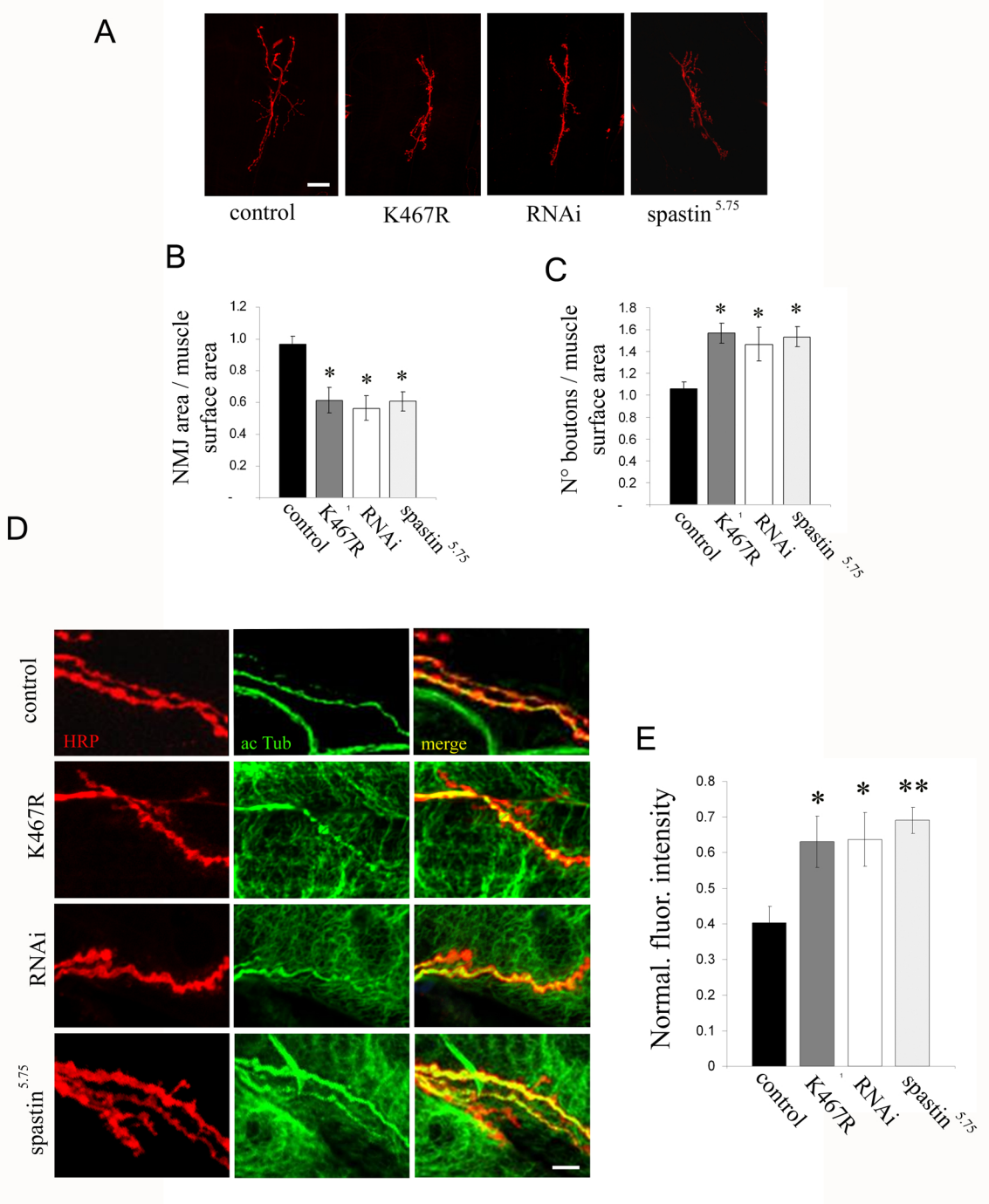
A
control
K467R
RNAi
spastin 5.75
B
NMJ area / muscle surface area
1.2
1.0
0.8
0.6
0.4
0.2
-
*
*
*
control
K467R
RNAi
spastin 5.75
C
N° boutons / muscle surface area
1.8
1.6
1.4
1.2
1.0
0.8
0.6
0.4
0.2
-
*
*
*
control
K467R
RNAi
spastin 5.75
D
control
K467R
RNAi
spastin 5.75
HRP
ac Tub
merge
E
Normal. fluor. intensity
0.8
0.7
0.6
0.5
0.4
0.3
0.2
0.1
0
*
*
**
control
K467R
RNAi
spastin 5.75

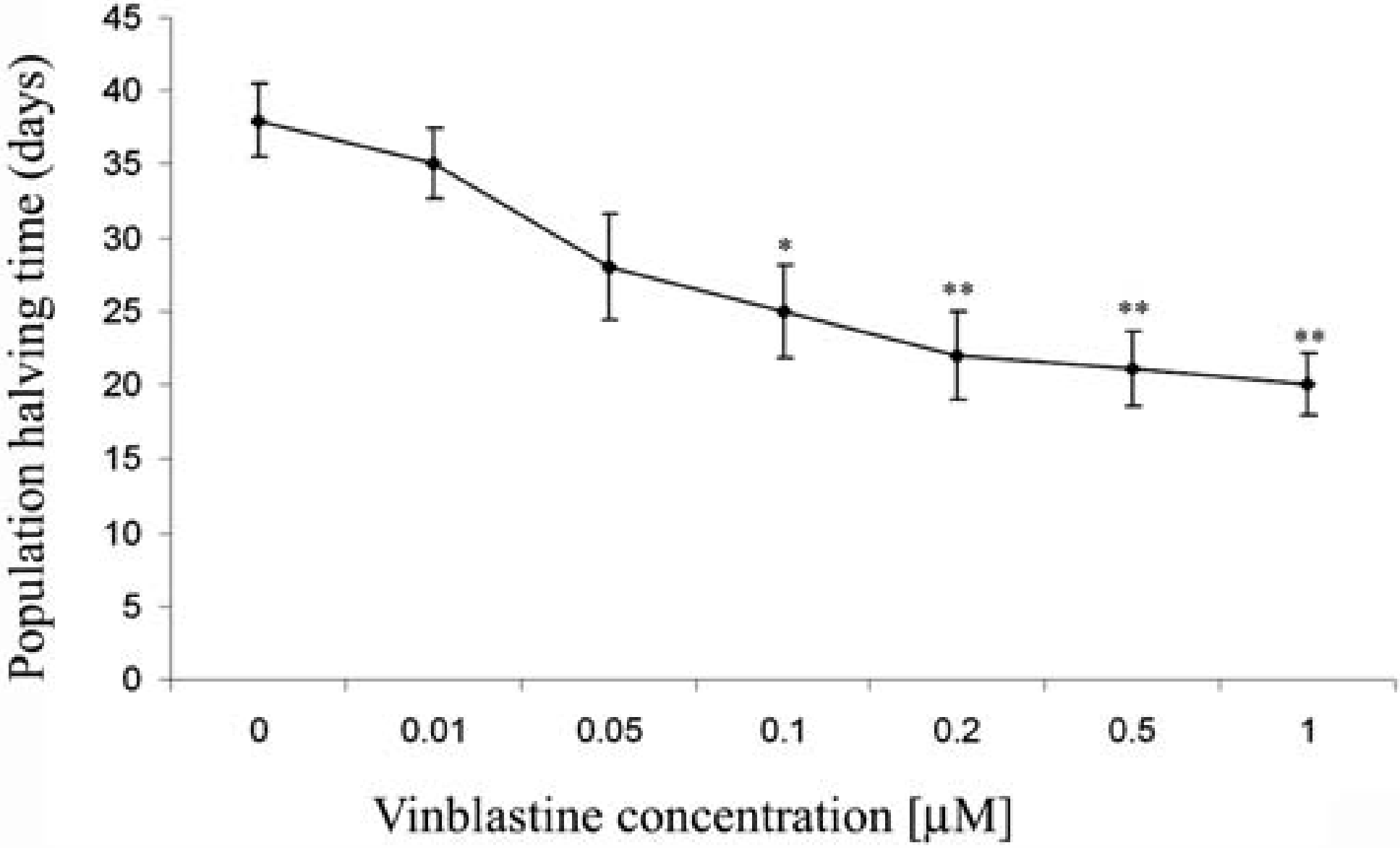
Population halving time (days)
45
40
35
30
25
20
15
10
5
0
*
**
**
**
0
0.01
0.05
0.1
0.2
0.5
1
Vinblastine concentration [µM]

***Supplemental data**

Supplemental Discussion

Dspastin RNAi and *Dspastin*$^{5.75}$ null flies exhibit analogous phenotypic alterations

Sherwood et al., 2004 have recently reported that Dspastin null mutants display phenotypes that are in sharp contrast to our observations. To resolve these discrepancies, we have carried out an extensive phenotypic comparison between our Dspastin RNAi and Dspastin K467R flies with Dspastin$^{5.75}$ null flies. A direct comparison of the results reported in this paper with those presented by Sherwood et al. is not possible because we have knocked down Dspastin specifically and exclusively in the nervous system while a null mutation such as that used by Sherwood et al. affects all tissues in which Dspastin is normally expressed. Thus, we have performed several experiments to compare flies ubiquitously expressing Dspastin RNAi and Dspastin K467R using the tubulin-gal4 driver and Dspastin$^{5.75}$ null mutants (Supplemental Figure 2). All phenotypes analyzed were consistently similar between Dspastin$^{5.75}$ null, Dpastin RNAi and Dspastin K467R flies, strongly supporting our conclusions that Dspastin negatively regulates microtubule stability and that its absence leads to the accumulation of stabilized microtubules and demonstrating that expression of both RNAi and K467R produce bona fide mutant phenotypes.

Figure legends

Supplemental Figure 1. Transgenic RNAi effectively and specifically reduces *Dspastin* expression. (**A**), RT-PCR showing loss of *Dspastin* mRNA in adult *Drosophila* brains following neuron specific expression of the *Dspastin* RNAi transgene (RNAi). Brains from Dspastin null and RNAi animals exhibit no change of control cDNA expression (2.5 kb band). The *Dspastin* message (2.1 kb band) is present in the w^{1118} control, but is undetectable in Dspastin null mutant (spastin$^{5.75}$) and elav-Gal4/+;UAS-RNAi/+ (RNAi) brains. (**B**), wild type *Drosophila* eye. (**C**), eyes expressing high levels of UAS-*Dspastin* under the control of the eye specific GMR-Gal4 driver display a severe small eye phenotype. (**D**), this small eye phenotype is completely suppressed by co-

expression of the RNAi construct by the same GMR-Gal4 driver line.

Supplemental Figure 2. Expression of *Dspastin* K467R produces neurodegeneration in the context of reduced *Dspastin* levels. (**A**), 18 day old fly heterozygous for Dspastin$^{5.75}$ shows no sign of neurodegeneration. (**B**), 20 day old fly with transgenic expression of *Dspastin* K467R has only modest neurodegeneration as indicated by a rare neuropil vacuole (arrow). (**C**), 18 day old fly with transgenic expression of *Dspastin* K467R in a Dspastin$^{5.75}$ heterozygous background has numerous vacuoles in the medulla (arrows) indicating increased levels of neurodegeneration. Scale bar is 10μm.

Supplemental Figure 3. Dspastin$^{5.75}$ null mutant flies and flies ubiquitously expressing Dspastin RNAi and Dspastin K467R display comparable phenotypic abnormalities. (**A**) confocal images of larval NMJ identified by HRP immunohistochemistry (red), show that in Dspastin$^{5.75}$/Dspastin$^{5.75}$, tub-Gal4/+; UAS-*Dspastin*-RNAi/+, and tub-Gal4/+; UAS-*Dspastin*-K467R /+ individuals, total NMJ area is similarly decreased and that synaptic boutons are smaller, more numerous and more clustered than in controls. Quantitative and statistical analyses of total synaptic area normalized to muscle size (**B**) and bouton number normalized to muscle size (**C**) indicate that these phenotypic variations are comparable among experimental genotypes and significantly different from controls (* $p<0.001$). (Scale bar represents approximately 20μM). (**D**) images of NMJ immunohistochemistry using an anti-HRP antibody (*red*), and an anti-acetylated α-tubulin antibody (green) that labels exclusively stable microtubules, demonstrate a similar accumulation of stabilized microtubules in Dspastin$^{5.75}$ / Dspastin$^{5.75}$, tub-Gal4/+; UAS-*Dspastin*-RNAi/+, and tub-Gal4/+; UAS-*Dspastin*-K467R /+ individuals, as indicated by the striking increase of acetylated tubulin signal, in comparison to controls; note that detector gain of the green channel for Dspastin$^{5.75}$ / Dspastin$^{5.75}$, tub-Gal4/+; UAS-*Dspastin*-RNAi/+, and tub-Gal4/+; UAS-*Dspastin*-K467R /+ has been reduced to 75% of that used to image controls to prevent signal saturation. (Scale bar

represents approximately 10μM). (**E**), quantitative and statistical analyses reveal that the increase in acetylated tubulin staining is comparable within experimental genotypes and significantly different from controls (* $p<0.001$, ** $p<0.0001$). Control genotypes: tub-Gal4/+, Dspastin$^{5.75}$/+.

Supplemental Figure 4. Effects of vinblastine on the lifespan of wild type Drosophila. Concentrations of 0.1 μM and above are associated with statistically significant levels of vinblastine induced lethality (* $p<0.001$, ** $p<0.0001$).